Prostaglandin E_2 Inhibits Renal Collecting Duct Na^+ Absorption by Activating the EP_1 Receptor

YouFei Guan,*¶ YaHua Zhang,*¶ Richard M. Breyer,*¶ Beth Fowler,*¶ Linda Davis,*¶ Richard L. Hébert,§‖ and Matthew D. Breyer*‡¶

**Division of Nephrology, Department of Medicine, ‡Department of Molecular Physiology and Biophysics, Vanderbilt University School of Medicine, Nashville, Tennessee 37212; §Department of Cellular Medicine and ‖Department of Molecular Medicine, University of Ottawa, Ottawa, Ontario, Canada K1H 8L6; and ¶Veterans Administration Medical Center, Nashville, Tennessee 37212*

Abstract

PGE_2 exerts potent diuretic and natriuretic effects on the kidney. This action is mediated in part by direct inhibition of collecting duct Na^+ absorption via a Ca^{++}-coupled mechanism. These studies examine the role the Ca^{++}-coupled PGE-E EP_1 receptor plays in mediating these effects of PGE_2 on Na^+ transport. Rabbit EP_1 receptor cDNA was amplified from rabbit kidney RNA. Nuclease protection assays demonstrated highest expression of EP_1 mRNA in kidney, followed by stomach, adrenal, and ileum. In situ hybridization, demonstrated renal expression of EP_1 mRNA was exclusively over the collecting duct. In fura-2–loaded microperfused rabbit cortical collecting duct, EP_1 active PGE analogs were 10–1,000-fold more potent in raising intracellular Ca^{++} than EP_2, EP_3, or EP_4-selective compounds. Two different EP_1 antagonists, AH6809 and SC19220, completely blocked the PGE_2-stimulated intracellular calcium increase. AH6809 also completely blocked the inhibitory effect of PGE_2 on Na^+ absorption in microperfused rabbit cortical collecting ducts. These studies suggest that EP_1 receptor activation mediates PGE_2-dependent inhibition of Na^+ absorption in the collecting duct, thereby contributing to its natriuretic effects. (*J. Clin. Invest.* 1998. 102:194–201.) Key words: rabbit • calcium • tubules • receptor antagonist • cloning

Introduction

PGE_2 is the major prostaglandin produced along the nephron, and the collecting duct displays the highest rates of segmental PGE_2 synthesis, where it potently regulates solute and water transport (1). The renal effects of PGE_2 have profound implications for the maintenance of glomerular filtration and sodium homeostasis, particularly in volume depletion and other states associated with decreased renal perfusion (2, 3). Conversely, in the elderly or in patients with mild renal insufficiency, chronic cyclooxygenase inhibition is associated with reduced urinary PGE_2 excretion, Na^+ retention, and hypertension, without measurable changes in glomerular filtration rate (4, 5). These observations suggest that cyclooxygenase inhibitors prevent the endogenous natriuretic and diuretic effects of renal PGE_2 and other prostanoids leading to expansion of extracellular fluid volume and hypertension.

The cellular and molecular basis of PGE-induced natriuresis is only partially understood. Previous studies in rabbit demonstrate that PGE_2 directly inhibits collecting duct Na^+ absorption (6). This effect is coupled to increased intracellular calcium ($[Ca^{++}]_i$)[1] via a pertussis toxin insensitive mechanism; however, the receptor mediating this effect remains uncharacterized (7). The cellular effects of PGE_2 are now known to be mediated by a subfamily of G protein–coupled receptors, designated EP receptors (for E-prostanoid; reference 8). Four distinct EP receptor subtypes, EP_1, EP_2, EP_3, and EP_4 have been cloned and expressed (9, 10). Each possesses a unique amino acid sequence, with differing affinity for PGE analogs and distinct signaling mechanisms (11). The EP_1 receptor signals predominantly via increased cell Ca^{++} and phosphatidylinositol-bisphosphate hydrolysis (12–14). Several EP_1 receptor selective antagonists have been characterized, which may be used to block its functional activation (11, 15). EP_2 and EP_4 receptors activate G_s and cAMP generation (8, 9, 16). Increased cAMP may also increase Ca^{++} in the collecting duct (17). Conversely EP_3 receptors act via G_i to inhibit cAMP generation (16, 18–22). However, multiple alternatively spliced EP_3 receptor variants exist that differ in their carboxy-terminal tail amino acid sequence (20, 23). These EP_3 splice variants display differential coupling to alternative signaling mechanisms including increased cAMP generation and phosphatidylinositol-bisphosphate hydrolysis (20).

Multiple EP receptor mRNAs have been detected in the kidney and these display distinct segmental localization along the nephron (9). EP_4 receptor mRNA is primarily expressed in the glomerulus, where it may contribute to the renal vasodilator effects of PGE_2 (16, 24). EP_4 receptors may also be present in the collecting duct (25). EP_3 receptor mRNA is highly expressed in the collecting duct and thick ascending limb, where it may mediate the effects of PGE_2 on salt and water transport (7, 9, 26, 27). In contrast, EP_1 receptor mRNA expression appears to be restricted to the collecting duct in both mouse and man (14, 24, 28). Little data exists for either mouse or man, regarding the role of collecting duct prostaglandin receptors in regulating ion transport. The existence of EP_1 receptor mRNA in the rabbit collecting duct has not been demonstrated, however given PGE_2 Ca^{++}-coupled signaling demonstrated there, it is a prime candidate for mediating inhibition of collecting duct Na^+ transport (7). These studies were designed to charac-

Address correspondence to Matthew D. Breyer, M.D., F-427 ACRE Bldg., Veterans Administration Medical Center, Nashville, TN 37212. Phone: 615-327-4751 ext. 5103; FAX: 615-343-7156. E-mail: Matthew.Breyer@mcmail.vanderbilt.edu

Received for publication 21 January 1998 and accepted in revised form 30 April 1998.

The Journal of Clinical Investigation
Volume 102, Number 1, July 1998, 194–201
http://www.jci.org

1. *Abbreviations used in this paper:* $[Ca^{++}]_i$, intracellular calcium; CCD, cortical collecting duct; J_{Na}, ^{22}Na flux; $J_{Na(l-b)}$, lumen-to-bath ^{22}Na flux; PKN, protein kinase N; RT, reverse transcription; V_o, collection rate.

terize the role of the EP_1 receptor in mediating PGE_2 inhibition of Na^+ absorption in the collecting duct.

Methods

Amplification and cloning of a rabbit EP_1 cDNA fragment

Reverse transcription–polymerase chain reaction (RT-PCR) was used to amplify a portion of the rabbit EP_1 receptor. Total RNA was purified from rabbit kidney and adrenal using TRIZOL-REAGENT™ (GIBCO BRL, Gaithersburg, MD) and reverse transcribed to single-stranded cDNA using SuperScriptII™ (reverse transcriptase and 0.5 μg of oligo$(dT)_{12–18}$ according to manufacturer's protocol. The cDNAs were then amplified using EP_1-selective primers. Primers were selected from conserved sequences in the putative second extracellular loop and transmembrane domain 7 of human, rat, and mouse EP_1 sequences (13, 14, 29). The sense primer was 5′-CTG CAG TAC CCG GGC ACG TGG TGC-3′ (see Fig. 1, Primer 1), and the antisense primer was 5′-CTG GCG CAG TAG GAT GTA CAC CCA-3′ (see Fig. 1, Primer 2; references 12–14, 29). PCR reactions were carried out using Advantage-GC™ cDNA PCR kit (Clontech, Palo Alto, CA) at 94°C for 0.5 min, 62°C for 3 min for 35 cycles in a Perkin-Elmer Cetus 9600 thermal cycler (Perkin-Elmer Cetus Instruments, Emeryville, CA). A 534-bp fragment was ligated into pCR™ II vector (Invitrogen Corp., San Diego, CA) and sequenced. The amplified cDNA fragment was homologous to the coding region of EP_1 of human, rat, and mouse (12–14, 29).

To obtain additional rabbit EP_1 cDNA sequence, two additional gene-specific sense primers were designed: an 18-mer 5′-CGC TGC TCG CCG CCC TCG-3′ (see Fig. 1, Primer 3) and an 18-mer 5′-CGC CTC GTC CGC CTC GTC-3′ (see Fig. 2, Primer 4). Rabbit kidney total RNA (1 μg) was reverse transcribed and the cDNA was used for amplification of additional 3′-EP_1 sequence using a 3′RACE system (3′ rapid amplification of cDNA ends) according to the manufacturer's specifications (GIBCO BRL). A resulting 582-bp product from primer 4 and the 3′RACE poly T/anchor primer contained a portion of the 3′ coding region and 3′ untranslated region (see Fig. 1) was cloned into pCRII vector (Invitrogen Corp.). A 3′ 223-bp NotI/EcoRI fragment of this EP_1 3′RACE product was further subcloned into pBlueScript SK(−) (Stratagene, Inc., La Jolla, CA) and used as a template to synthesize sense and antisense riboprobe for RNase protection assays.

Solution hybridization/RNase protection assays

RNase protection assays were performed as previously described (30). Briefly, the plasmids (pBluescript SK−) containing rabbit EP_1 fragment were linearized with appropriate restriction enzymes. Radioactive riboprobes were synthesized from 1 μg of linearized plasmids in vitro by using MAXIscript™ kit (Ambion, Inc., Beverly, MA) for 1 h at 37°C in a total volume of 20 μl. The reaction buffer contained 10 mM DTT, 0.5 mM ATP, CTP, and GTP, 2.5 μM of UTP, and 5 μl of 800 Ci/mmol [α-^{32}P] UTP at 10 mCi/ml (DuPont-NEN, Boston, MA). Hybridization buffer included 80% deionized formamide, 100 mM sodium citrate, pH 6.4, and 1 mM EDTA (RPA II, Ambion, Inc.). 50 μg of total RNA isolated from various rabbit tissues using TRIZOL-REAGENT™ (GIBCO BRL) were incubated at 45°C for 12 h in hybridization buffer with 5×10^4 cpm labeled riboprobes. After hybridization, ribonuclease digestion was carried out at 37°C for 30 min, and protected fragments were precipitated and separated on 4% polyacrylamide gel at 200 V for 3 h. The gel was exposed to Kodak XAR-5 film (Eastman Kodak Co., Rochester, NY) overnight at −80°C with intensifying screens.

In situ hybridization and localization of the EP_1 receptor cDNA

In situ hybridization was performed as previously described (30). Briefly, before hybridization, rabbit kidney sections were deparaffinized, refixed in paraformaldehyde, treated with proteinase K (20 μg/ml), washed with PBS, refixed in 4% paraformaldehyde, and treated with triethanolamine plus acetic anhydride (0.25% vol/vol). Finally, sections were dehydrated with 100% ethanol. ^{35}S-labeled antisense and sense riboprobes from rabbit EP_1 were hybridized to the section at 55°C for 18 h. After hybridization, the sections were washed at 65°C once in 5× SSC plus 10 mM β-mercaptoethanol, once in 50% formamide, 2× SSC, and 100 mM β-mercaptoethanol for 30 min. After an additional two washes in 10 mM Tris, 5 mM EDTA, 500 mM sodium chloride at 37°C, sections were treated with RNase A (10 μg/ml) at 37°C for 30 min, followed by another wash in 500 mM sodium chloride at 37°C. Sections were then washed twice in 2× SSC, and twice in 0.1× SSC at 65°C. Slides were dehydrated with graded ethanol containing 300 mM ammonium acetate. Slides were then dipped in emulsion (Ilford K5; Knutsford, Cheshire, United Kingdom) diluted 1:1 with 2% glycerol, and exposed for 4–5 d at 4°C. After developing in Kodak D-19, slides were counterstained with hematoxylin. Photomicrographs were taken using a Zeiss Axioskop microscope (Carl Zeiss, Inc., Thornwood, NY) and either dark-field (Micro Video Instruments, Avon, MA) or bright field optics.

General microperfusion methods

In vitro microperfusion of isolated CCDs was performed as previously described (26). Female New Zealand white rabbits weighing 1.5–2.5 kg were killed using an intramuscular injection of ketamine (44 mg/kg) and xylazine (11 mg/kg) for anesthesia followed by decapitation. The left kidney was quickly removed, and 1–2 mm coronal slices were placed in chilled dishes for freehand microdissection. Single CCDs were transferred to a thermostatically controlled chamber of 1 ml volume and cannulated using concentric micropipettes. Bath solution was continuously exchanged at 0.5 ml/min by infusion pump (Sage; Orion Research, Cambridge, MA) and was maintained at 37°C. Transepithelial voltage was measured via a Ringer's agarose bridge connected to the perfusion pipette and a calomel electrode. A similar bridge connected the bath to another calomel electrode and completed the circuit. Transepithelial voltage, in mV, was measured with an electrometer (FD223; WPI, Inc., Sarasota, FL) and continuously recorded on a strip-chart recorder (Primeline model R-02; Soltec Co., Sun Valley, CA). The composition of standard bath medium, dissection medium, and isotonic perfusate were as follows (in millimole): NaCl, 105; $NaHCO_3$, 25; Na acetate, 10; Na_2HPO_4, 2.3; KCl, 5; $CaCl_2$, 1.8; $MgSO_4$, 1.0; glucose, 8.3; and alanine, 5; (osmolality ∼ 300 mOsmol).

^{22}Na flux in isolated perfused CCDs

CCDs were perfused at 2–3 nl/min. ^{22}Na (25 μCi/ml; DuPont-NEN) and [^{3}H]inulin (75 μCi/ml) were added to the perfusate which was otherwise identical to the bath. After a 90–105-min equilibration, three control collections were made into a pipette of predetermined volume (between 25 and 40 nl) to measure basal lumen-to-bath ^{22}Na flux (J_{Na}). In some studies, an EP_1 receptor antagonist (either AH6809 or SC19220, 10 μM) was added to the bath and after a 10-min equilibration period, three additional timed collections were made. The effect of 30 nM PGE_2 on J_{Na} was determined in the presence or absence of the EP_1 antagonist. J_{Na} was defined as the mean of the final three collections made during exposure to the different agonists used. Changes in lumen-to-bath J_{Na} previously have been shown to reflect changes in net sodium absorption, since bath-to-lumen J_{Na} is low and unaffected by PGE_2 (6, 31). A final period of J_{Na} measurements was performed in the presence of bath 10^{-4} M ouabain. Ouabain inhibits net J_{Na} close to zero, thus residual lumen-to-bath J_{Na} postouabain is passive and comparable to bath-to-lumen J_{Na} (31).

Measurement of $[Ca^{++}]_i$ in isolated perfused tubules (CCDs)

CCDs were perfused in vitro as described above with the following differences: the bath was a special low volume (0.150 ml) chamber to allow for rapid fluid exchange (32, 33). The bath solution was preheated in a water-jacketed line and flow rate was maintained between 0.5–2.5 ml/min. Before loading with fura-2, CCD autofluorescence and background were determined (typically < 20% of fluorescent

emission in fura-2–loaded tubules). This value was continuously subtracted from all subsequent measurements. CCDs were bathed with 2.5 μM acetoxymethyl ester of fura-2 (fura-2-AM; Molecular Probes, Inc., Eugene, OR) for 45 min at 30°C. After tubules were loaded, the bath temperature was increased to 37°C, the flow rate was increased to 2.5 ml/min and tubules were allowed to equilibrate for 20–30 min. Fluorescence excitation was accomplished using continuous rapidly alternating illumination (20 ms per reading) from dual monochromators set at 340 and 380 nm, respectively (Deltascan; Photon Technology International, Monmouth Junction, NJ). The monochromator output was coupled to an inverted microscope using a 400-nm dichroic mirror and a ×100 lens (n.a. 1.3; Nikon fluor oil immersion; Nikon, Inc., Melville, NY). Fluorescent emission of wavelengths > 435 nm was measured by photon counting using a long pass filter. The emission slit encompassed a 100× 40 μm rectangle oriented along the long axis of the tubule. This area is estimated to include ~ 100 cells. Using 340 and 380 nm excitation (340/380 ratio, R), the emission intensity ratio (corrected for background) was continuously monitored.

In situ calibration of $[Ca^{++}]_i$ was performed at the end of each experiment. The bath medium was changed to a Ca^{++}- and Mg^{++}-free isotonic bath medium containing 2 mM EGTA and 10 μM 4Br-A23187. After a stable III40/380 ratio (minimum ratio) was achieved the bath was changed back to normal bath medium (2.4 mM Ca^{++}) and 10 μM of 4Br-A23187 and the ratio was again allowed to stabilize (maximum ratio).

Calculations

Sodium transport. Jv was uniformly < 1% of the collection rate (V_o), allowing the perfusion rate be taken as equal to the collection rate V_o. $J_{Na(l-b)}$ was calculated as previously described in reference 7: $J_{Na(l-b)} = (1 - C^*_o/C^*_i) \times 145 \times V_o$/liter = pmol/mm per minute. C^*_i and C^*_o are perfused and collected fluid concentrations of ^{22}Na (cpm/nl). The basal Na^+ transport rate for each CCD was normalized to the group's average basal transport rate as follows: the overall average basal J_{Na} for each group was divided by the basal J_{Na} of an individual tubule; this unique fraction was then used to multiply the measured J_{Na} for each collection for that tubule. The result minimizes tubule-to-tubule variability in initial transport rates, thereby allowing the subsequent change in J_{Na} after the EP_1 antagonist or PGE_2 to be more clearly seen after averaging the data.

$[Ca^{++}]_i$. $[Ca^{++}]_i$ was estimated according to the standard formula: $[Ca^{++}]_i = K_d (R - R_{min}) / (R_{max} - R)$ (380 min/380 max) where R_{min} is the minimum ratio and R_{max} is the maximum ratio, and assuming that the K_d value for the fura-2–Ca^{++} complex is 224 nM at 37°C (34).

Statistics

Data are presented as mean±SEM and statistical analyses were made using paired Student's *t* test or one-way ANOVA where appropriate. Differences with $P < 0.05$ were considered statistically significant.

Reagents

AVP, EGTA, PGE_2, and Pertussis toxin were purchased from Sigma Chemical Co. (St. Louis, MO). Fura-2-AM and 4Br-A23187 were purchased from Molecular Probes, Inc. Sulprostone was a generous gift from Berlex Laboratories, Inc. (Cedar Knolls, NJ). SC19220 was the generous gift of Searle Pharmaceuticals (Skokie, IL) and AH6809 was generously provided by Dr. R. Coleman (Glaxo Research Group, Ltd., Greenford, Middlesex, United Kingdom).

Results

Cloning and tissue expression of the rabbit EP_1 receptor mRNA. Two overlapping PCR products generated from rabbit kidney RNA were sequenced: a 534-bp RT-PCR product

A

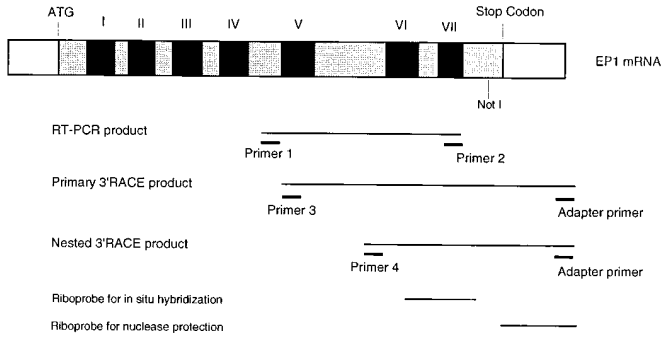

B

```
                193         207         222         237         250
human           GPPGGWRQALLAGLF ASLGLVALLAALVCN TLSGLALHRARWRRR S--RRPPPASGPDSR RRWGAHGPRSASASS    265
                193         207         222         237         250
rabbit          GPSRGWRQALLAGLF AGLGLAALLAALVCN TLSGLALLRARWRRR LSSRRLPQAAGPDSR RRWGARGTRSASASS
                193         207         222         237         250
mouse           GPRGGWRQALLAGLF AGLGLAALLAALVCN TLSGLALLRARWRRR RS-RRFRKTAGPDDR RRWGSRGPRLASASS    268
                195         209         224         239         253

                266         280         295         310         325
human           ASSIASASTFFGGSR SSGSARRARAHDVEM VGQLVGIMVVSCICW SPMLVLVALAVGGWS STSLQRPLFLAVRLA    340
                266         280         295         310         325
rabbit          ASSITSASAAFRGSR SGGSARRARAHDVEM MGQLVGIMVVSCICW SPLLVLVVLAVGGWS PSSLQRPLFLAVRLA
                266         280         295         310         325
mouse           ASSITSATATLRSSR GGGSARRVHAHDVEM VGQLVGIMVVSCICW SPLLVLVVLAIGGWN SNSLQRPLFLAVRLA    343
                269         283         298         313         328

                341         355         370         385         400
human           SWNQILDPWVYILLR QAVLRQLLRLLPPRA GAKGGPAGLGLTPSA WEASSLRSSRHSGLS HF    402
                341         355         370         385         400
rabbit          SWNQILDPWVYILLR QAVLRQLLRLLPPRA GAKGGRAELGLTRSA WEVSSLRSSRHSGLS HF
                341         355         370         385         400
mouse           SWNQILDPWVYILLR QAMLRQLLRLLPLRV SAKGGPTELGLTKSA WEASSLRSSRHSGFS HL    405
                344         358         373         388         403
```

Figure 1. Amplification of rabbit EP_1 receptor cDNA. (*A*) The regions of the rabbit EP_1 receptor amplified by RT-PCR and 3′RACE and areas used to generate riboprobes for nuclease protection and in situ hybridization. (*B*) The region of the amplified rabbit EP_1 cDNA was aligned with full length human and mouse sequences. The numbering corresponds to the residues for the human and murine amino acid sequences respectively. The cDNA sequence for the rabbit EP_1 receptor has been assigned GenBank accession number AF043491.

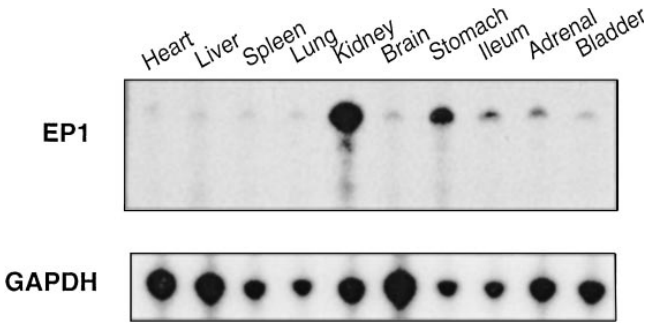

Figure 2. Distribution of rabbit EP_1 mRNA in normal rabbit tissues. A 223-nt EP_1 riboprobe complementary to portions of the 3′ coding and untranslated region was allowed to hybridize to 50 μg of total RNA from the indicated tissues. RNA loading was normalized using a riboprobe complementary to rabbit glyceraldehyde-3-phosphate dehydrogenase (*GAPDH*). The autoradiogram is representative of three separate experiments.

(using primers 1 and 2) and a 582-bp 3′RACE product (using primer 4 and a 38-bp poly-T/anchor 3′RACE primer). Excluding primer sequence, 759 bp of unique (nonoverlapping) rabbit EP_1 receptor sequence was obtained. Fig. 1 shows the predicted amino acid sequence for this cDNA which, when aligned to human and mouse EP_1 sequences (12, 13), is predicted to comprise a 212–amino acid region of the rabbit EP_1 receptor, homologous to the region downstream of the second extracellular loop. The predicted amino acid sequence is 87.3% and 84.4% identical to human (13) and mouse EP_1 sequences, respectively (14). Tissue distribution of rabbit EP_1 receptor mRNA was determined by nuclease protection assay. EP_1 mRNA level was highest in kidney, followed by stomach, ileum, and adrenal. Only faint expression of EP_1 receptor mRNA was detected in heart, liver, spleen, lung, brain, and urinary bladder (Fig. 2).

Intrarenal localization of rabbit EP_1 mRNA. In situ hybridization was used to examine the intrarenal distribution of EP_1 receptor mRNA. A 160-nt EP_1 antisense riboprobe comprising a region from the putative 3′ coding region of the EP_1 receptor was used. Outer medullary labeling and papillary labeling was greater than that in the cortex, consistent with the relative density of collecting duct in these regions of the kidney. EP_1 mRNA was not detected in glomeruli or other nephron segments (Fig. 3).

EP_1-selective prostaglandin analogs preferentially increase intracellular Ca^{++} in microperfused rabbit CCDs. To determine whether EP_1 receptor–dependent signaling is present in

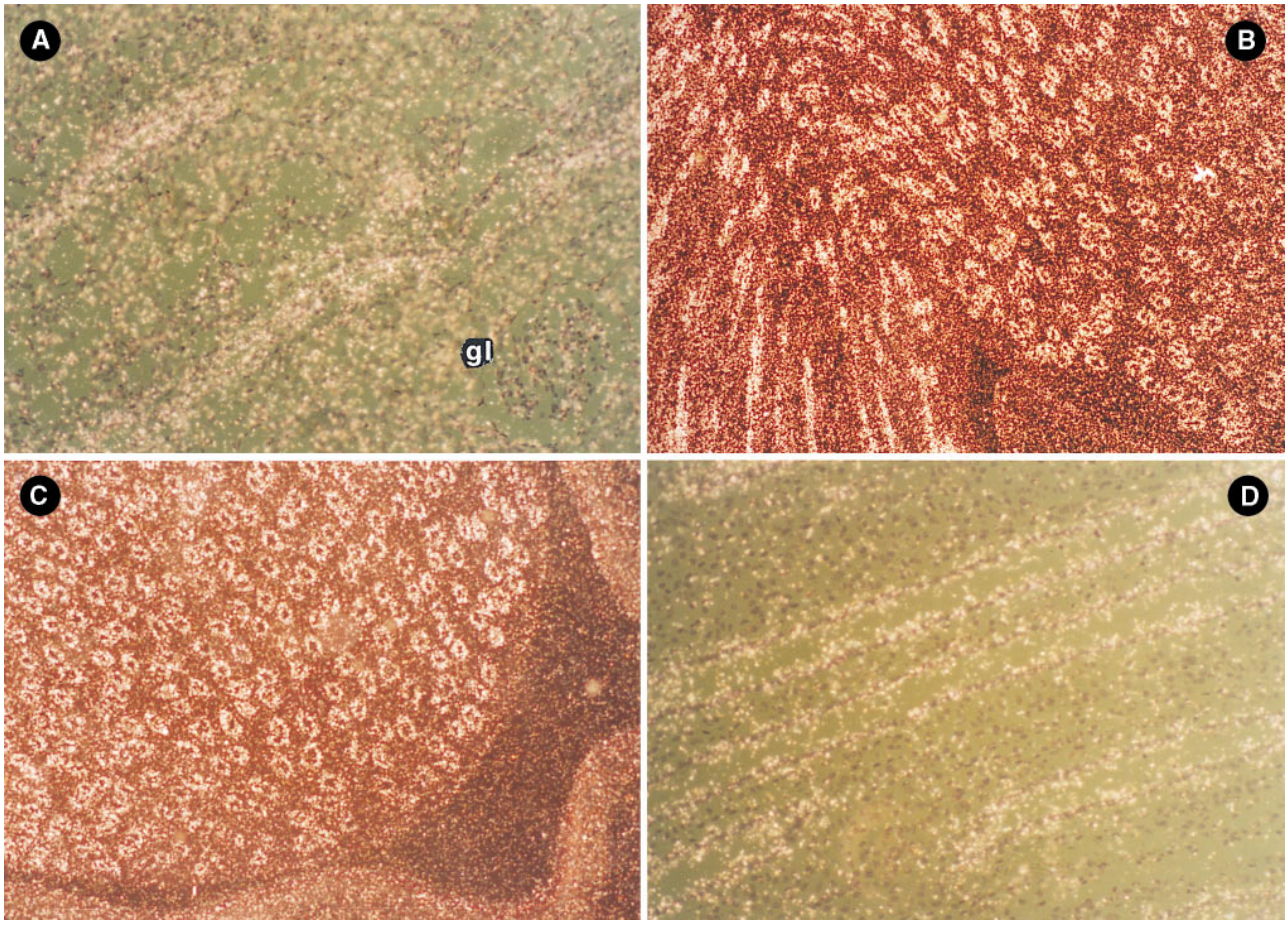

Figure 3. Intrarenal distribution of rabbit EP_1 mRNA was determined by in situ hybridization. (*A*) Simultaneous bright-field/dark-field exposure of the renal cortex (×200), where the white grains are localized over collecting duct, whereas glomeruli (*gl*) are unlabeled. (*B* and *C*) ×50 dark-field photomicrographs of renal outer medulla and papilla, respectively. The areas of radioactive EP_1 riboprobe hybridization are seen as white grains in the overlying photoemulsion refracting the tangential light from the dark-field illumination source. (*D*) ×200 bright-field/dark-field photomicrograph of renal medulla.

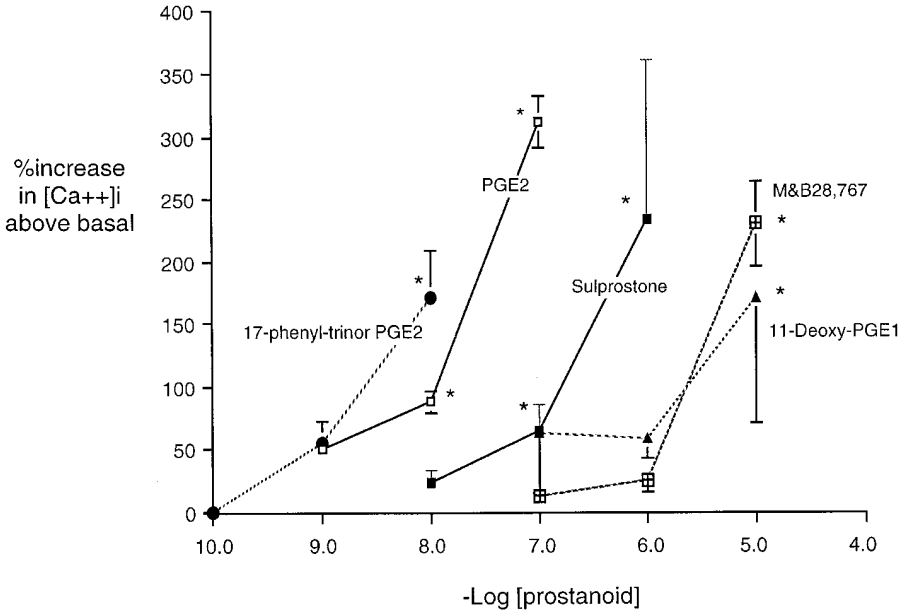

Figure 4. Effect of EP receptor agonists on $[Ca^{++}]_i$ in microperfused rabbit CCDs. PGE_2 and the $EP_{1/3}$ selective agonists 17phenyltrinor-PGE_2 and sulprostone were the most potent agonists studied. The $EP_{3/4}$-selective agonist 11-deoxy-PGE_1 and the EP_3-selective agonist MB28767 were the least potent agonists studied. Each data point represents the mean of at least three separate experiments±SEM. $*P < 0.05$ versus baseline Ca^{++}.

the collecting duct, we characterized the activity profile of EP receptor selective PGE-E analogs on $[Ca^{++}]_i$ in fura-2–loaded cortical collecting ducts (Fig. 4). The EP_1 agonist 17-phenyltrinor-PGE_2 was the most potent compound tested, significantly increasing $[Ca^{++}]_i$ from 187±41 to 327±45 nM using a concentration of 10 nM ($n = 8$; $P < 0.05$, ANOVA). Another $EP_{1/3}$ selective agonist, sulprostone, was at least 10-fold less potent than 17-phenyltrinor-PGE_2, requiring 100 nM concentrations to significantly increase CCD $[Ca^{++}]_i$. Neither EP receptor agonist is completely specific for the EP_1 receptor, and each displays significant affinity for the EP_3 receptor (35); however, the potent EP_3-selective agonist, MB28767, was among the weakest EP-selective analogs tested ($n = 4$), requiring concentrations of 10 μM or more to significantly increase CCD $[Ca^{++}]_i$. Similarly, the $EP_{3/4}$-active agonist 11-deoxy-PGE_1 only increased $[Ca^{++}]_i$ at concentrations of 1–10 μM ($n = 6$ and 3, respectively). Butaprost (10 μM), an EP_2 selective agonist, was completely without effect ($\Delta[Ca^{++}]_i = 7.6\pm4\%$, $n = 4$, ns). Fi-

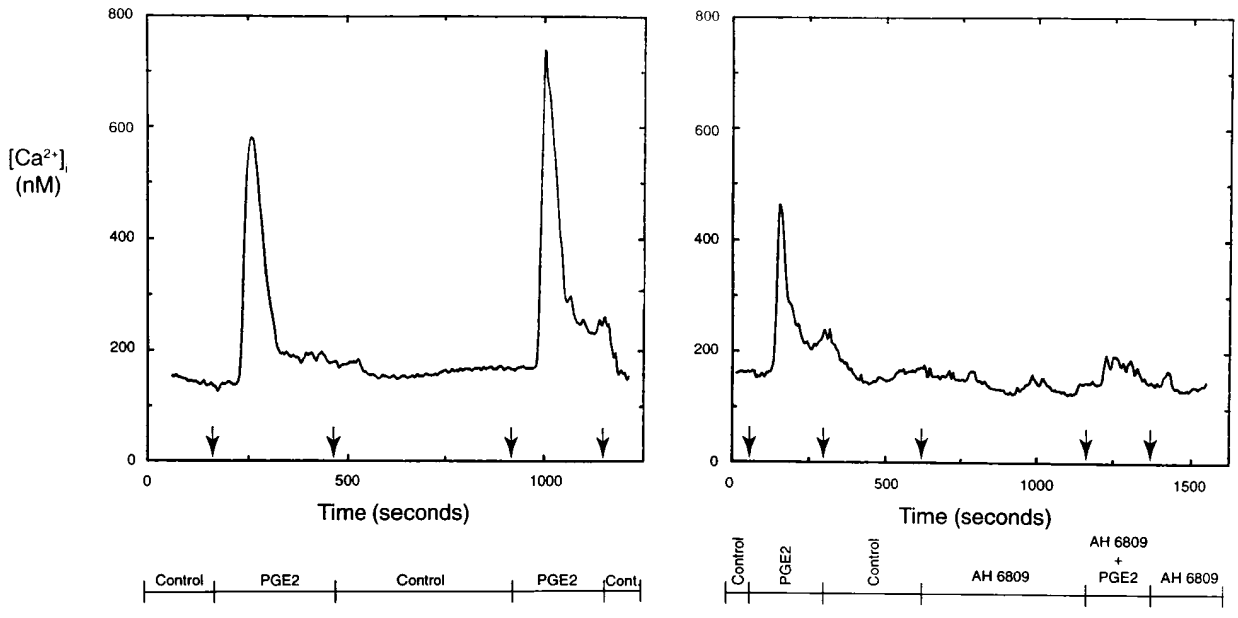

Figure 5. The effect of the EP_1 receptor antagonist on the PGE_2-induced $[Ca^{++}]_i$ increase. $[Ca^{++}]_i$ was measured in fura-2–loaded, microperfused rabbit collecting ducts. The left panel shows the effect of PGE_2 (30 nM) on $[Ca^{++}]_i$ over ~ 300 s. After a 10-min washout period, subsequent retreatment produced a second $[Ca^{++}]_i$ increase indistinguishable from the first. The right panel shows a representative tracing from another CCD where a similar $[Ca^{++}]_i$ is seen after the initial exposure to PGE_2. Subsequent exposure to 10 μM AH6809 had no effect on $[Ca^{++}]_i$, but it completely blocked the effect of the second PGE_2 treatment.

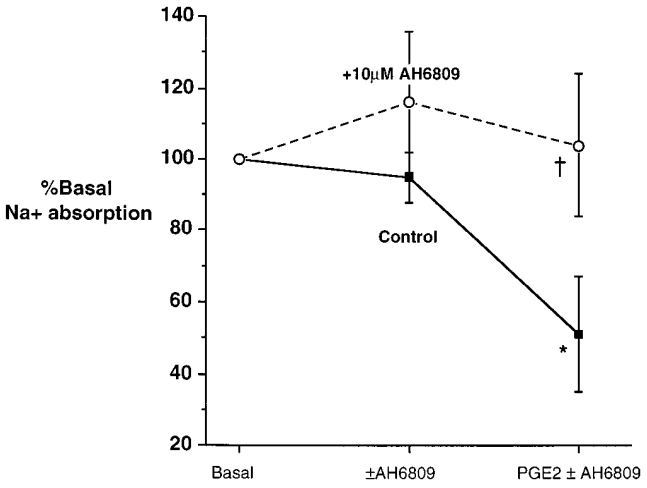

Figure 6. EP_1 receptor antagonist blocks PGE_2 inhibition of cortical collecting duct Na^+ absorption. Continuous measurements of $^{22}Na^+$ flux were made under control conditions, followed by AH6809 (10 μM) versus a second control period, followed by PGE_2 (30 nM) in the presence of AH6809 (*circles*) or its absence (*squares*). $^*P < 0.001$ PGE_2 alone versus control period; $^\dagger P < 0.005$ PGE_2 + AH6089 versus PGE_2 alone, ANOVA.

nally, although 100 nM $PGF_{2\alpha}$ significantly increased $[Ca^{++}]_i$, 1 mM fluprostenol, an FP receptor agonist (36), was completely without effect on CCD $[Ca^{++}]_i$ ($\Delta[Ca^{++}]_i = 28\pm19\%$, $n = 5$, ns).

EP_1 antagonists block the PGE_2-stimulated Ca^{++} increase in rabbit CCDs. To examine the effect of EP_1 receptor antagonists on $[Ca^{++}]_i$, a protocol was established allowing repeated effects of PGE_2 to be studied in the same tubule in the presence and absence of the antagonist. A concentration of PGE_2 was first identified that reproducibly increased $[Ca^{++}]_i$ in the microperfused CCD, but which was below the maximally effective concentration (Fig. 4). 30 nM PGE_2 increased CCD $[Ca^{++}]_i$ by 264±50 nM from basal values of 112±15 to 376±47 nM (peak 1, $n = 6$). After a 15-min washout period, re-exposure of the same CCD to 30 nM PGE_2 produced an identical change in $[Ca^{++}]_i$ (Table I, peak 2, $\Delta = 267\pm62$ nM, Fig. 5). In a separate group of studies, CCDs were initially exposed to 30 nM PGE_2, followed by a washout period during which the EP_1 receptor antagonist AH6809 was added, followed by re-addition of PGE_2. The initial treatment with PGE_2 increased $[Ca^{++}]_i$ by 207±27 nM ($n = 5$, Table I, peak 1, Fig. 5). After PGE_2 washout, 10 mM AH6809, did not change $[Ca^{++}]_i$ by itself; however, AH6809 markedly suppressed the subsequent increase in $[Ca^{++}]_i$ expected after re-exposure to 30 nM PGE_2. In the presence of AH6809, PGE_2 increased $[Ca^{++}]_i$ by only 47±5 nM ($P < 0.005$, Table I, peak 2 versus peak 1, ANOVA, Fig. 5). Similar results were obtained in unpaired studies with a structurally dissimilar EP_1 receptor antagonist, SC19220 (Table I). Pretreatment of microperfused CCDs with 10 μM SC19220 reduced the PGE_2 $[Ca^{++}]_i$ increase to only 90±20 nM from 264±50 nM ($n = 4$, $P < 0.05$). Thus two different EP_1 receptor antagonists, SC19220 and AH6809, blocked the PGE_2-stimulated Ca^{++} increase.

EP_1 receptor antagonism blocks inhibition of CCD Na^+ absorption by PGE_2. In control experiments, bath PGE_2 (30 nM) reduced lumen-to-bath ^{22}Na flux ($J_{Na\,l-b}$) from control rates of 57.2±10.8 to 41.4±9.5 pmol × mm^{-1} × min^{-1} ($n = 5$, $P < 0.005$ ANOVA). PGE_2-dependent inhibition of $J_{Na(l-b)}$ was completely blocked by pretreating CCDs with the EP_1 receptor antagonist AH6809. In the presence of 10 μM AH6809, 30 nM PGE_2 failed to significantly inhibit J_{Na}, with control rates of 33.3±4.5 pmol × mm^{-1} × min^{-1} remaining at 31.2±4.8 after 30 nM PGE_2 ($n = 6$, $P > 0.1$, ANOVA). Furthermore, by itself, AH6809 had no effect on J_{Na} (control 30.1±3 pmol/mm per minute to 10 μM AH6809 33.3±4.4). Ouabain inhibited ^{22}Na efflux to 17.6±3.3 pmol × mm^{-1} × min^{-1}, or to 41±4.2% of basal rates. Inhibition of $J_{Na(l-b)}$ by PGE_2 represents a 49±16% reduction in the ouabain-sensitive component of lumen-to-bath ^{22}Na flux (Fig. 6), an estimate of its effect on active Na^+ absorption in the CCD.[2] These studies demonstrate

2. Previous studies in rabbit CCD show PGE_2 has no effect on passive bath-to-lumen flux of isotopic Na^+ (6) and that postouabain $J_{Na\,l-b}$ is a good estimate of passive $^{22}Na^+$ permeability (31). Thus, the ouabain sensitive component of $J_{Na\,l-b}$ reflects active transport and is the component affected by PGE_2.

Table I. Effect of EP_1 Receptor Antagonists on PGE_2-stimulated Ca^{++} Increase in Collecting Ducts

A. Protocol No.	Condition	$\Delta[Ca^{++}]$, nM	*n*	*P* value
1	PGE2 (30 nM)	263±49.7	6	—
2	SC19220 (10 μM) + PGE2 (30 nM)	90.4±20*	4	$^*P < 0.05$, No. 1 vs. 2
3	AH6809 (10 μM) + PGE2 (30 nM)	76.1±37.3*	4	$^*P < 0.05$, No. 1 vs. 3

B. Protocol	$\Delta[Ca^{++}]$i, nM		*n*	*P* value
	(1) 30 nM PGE_2	(2) 30 nM PGE_2±AH6809		
Period No.				
Time controls	263.7±49.7	267.4±62.1	6	ns, 1 vs. 2
AH6809 (10 μM)	207.1±27.1	47.2±5.4‡	5	‡$P < 0.005$, No. 1 vs. 2

(*A.*) Effect of PGE_2 on cell calcium in the presence or absence of EP_1 receptor agonists. (*B.*) Sequential effects of PGE_2 on cell calcium (±AH6809). *One-way ANOVA; ‡paired Student's *t* test.

that the EP_1 receptor antagonist AH6809 blocks PGE_2 inhibition of collecting duct Na^+ absorption.

Discussion

Renal prostaglandins play a critical role in maintaining Na^+ balance (2, 37). PGE_2 is the major prostaglandin synthesized along the rabbit nephron (1) and is a major urinary prostanoid (38). Intrarenal PGE infusion results in a natriuresis and diuresis, without significant changes in glomerular filtration rate, supporting its role as a natriuretic autacoid that modulates epithelial Na^+ absorption (39). A direct inhibitory effect of PGE_2 on Na^+ transport in in vitro microperfused collecting ducts has been well established by numerous studies performed over the past two decades (6, 7, 40). More recent studies suggest the mechanism by which PGE_2 inhibits collecting duct Na^+ absorption is coupled to increased cell Ca^{++} and can be blocked by reducing extracellular Ca^{++} into the nanomolar range (7). This is consistent with the well-known inhibitory effect of increased cell Ca^{++} on collecting duct Na^+ absorption, although the mechanism of this effect appears to be indirect and not a result of direct interaction of Ca^{++} with the epithelial Na^+ channel (41–43). These studies now demonstrate that the prostaglandin EP_1 receptor is expressed in the rabbit collecting duct and suggest it plays a crucial role in mediating both the PGE_2 mediated increase in Ca^{++} and inhibition of Na^+ absorption in this segment.

Evidence from several species suggests all four EP prostanoid receptor subtypes (EP_1, EP_2, EP_3, and EP_4) are expressed in the kidney (12, 14, 16, 24, 28, 29, 44, 45). This paper demonstrates that as opposed to the rabbit EP_3 and EP_4 receptors (16, 45), renal expression of EP_1 receptor mRNA in rabbit is exclusively detected in the collecting duct. It is intriguing that the EP_1 receptor mRNA also displays a relatively restricted tissue distribution, being mainly expressed in the kidney with lower expression levels in stomach. Our use of nuclease protection rather than cDNA probes and Northern hybridization may be a more reliable means of characterizing EP_1 mRNA expression levels, given the recent realization that protein kinase N (PKN) mRNA is transcribed from the DNA antiparallel to the EP_1 gene (46). PKN mRNA is expressed in several tissues and EP_1 cDNA probes could also hybridize to this message, making Northern results more difficult to interpret (29). Nevertheless EP_1 receptor RNA expression also appears to be greatest in mouse (12) and human kidney (47), while results in rat are less clear-cut (29). The restricted expression of the EP_1 mRNA is in contrast to other EP receptors that show high mRNA expression levels in several tissues (16, 23, 45). Low levels of EP_1 mRNA expression in stomach, adrenal, and brain may not reflect a lack of a functional significance in these tissues. EP_1 receptor expression may be limited to discrete but physiologically critical regions, including hypothalamus (14) and gastrointestinal muscularis mucosa (48) where EP_1 may play roles in fever and intestinal motility, respectively (15, 49).

While studies in mouse and man also demonstrate that renal EP_1-receptor mRNA is restricted to the collecting duct, these studies in rabbit uniquely allowed complementary characterization of EP receptor transport effects in microperfused nephron segments in parallel with receptor distribution (14, 24, 28). These data suggest the EP_1 receptor mediates the PGE_2-stimulated Ca^{++} increase in the rabbit CCD. The low potency of MB28767 and 11-deoxy-PGE_1 argue against the Ca^{++} increase being mediated via an EP_3 receptor, since these analogs bind to, and activate, the EP_3 receptor in nanomolar concentrations (20, 23, 50, 51), but have $\sim$ 100-fold lower affinity for the EP_1 receptor (35). Namba et al. (20) have suggested that activation of certain EP_3 receptor COOH-terminal splice variants with MB28767 may activate phosphatidylinositol hydrolysis and raise cell Ca^{++} via both pertussis sensitive and insensitive pathways. Several EP_3 splice variants appear to exist in rabbit kidney (23); however, the low potency of MB28767 argues against their role in mediating the Ca^{++} increase in rabbit collecting duct. 11-deoxy-PGE_1 also potently binds to and activates the EP_4 receptor (16, 25, 35), so its poor activity also argues against an EP_4 receptor mediating this effect. Similarly, Butaprost was without effect, arguing against an EP_2-mediated action. Only ligands with EP_1 receptor activity (i.e., sulprostone and 17-phenyltrinor-PGE_2 [8, 35]) increased CCD $[Ca^{++}]_i$ when used in submicromolar concentrations.

A central role for the EP_1 receptor in mediating the Ca^{++}-dependent inhibition of Na^+ absorption in the collecting duct was further substantiated by the demonstration that two different EP_1 receptor antagonists, AH6809 and SC19220, completely blocked both the PGE_2-stimulated Ca^{++} increase and inhibition of Na^+ absorption. Relatively high concentrations of AH6809 and SC19220 were required to block these effects, consistent with the relatively low potency of these antagonists, with IC_{50} values of 0.5 and 6.7 μM for the cloned human EP_1 receptor (13). Importantly, at these concentrations, neither receptor antagonist acted as an agonist in rabbit collecting duct, producing no change in baseline $[Ca^{++}]_i$, or $^{22}Na^+$ flux. While these compounds show reasonable in vitro activity, their in vivo utility is limited by this low potency, low water solubility, and avid binding to plasma proteins (11, 15). Thus, characterization of the in vivo effects of EP_1 antagonists on Na^+ balance awaits the availability of improved EP_1 receptor antagonists. It remains to be determined whether decreased PGE_2-dependent EP_1 receptor activation contributes to the Na^+ retention observed with cyclooxygenase inhibitors in vivo (5).

In summary, these studies provide both molecular and functional evidence for the presence of an EP_1 receptor in the rabbit collecting duct. Rabbit EP_1 receptor RNA distribution is predominantly detected in the kidney where it is restricted to the collecting duct. Activation of the collecting duct EP_1 receptor increases $[Ca^{++}]_i$, while EP_1 receptor antagonists block both this Ca^{++} increase and PGE_2's capacity to inhibit Na^+ absorption. These results suggest EP_1 receptor activation contributes to the natriuretic effects of PGE_2.

Acknowledgments

Sulprostone was a generous gift from Berlex Laboratories, Inc. (Cedar Knolls, NJ). SC19220 was the generous gift of Searle Pharmaceuticals (Skokie, IL) and AH6809 was generously provided by Dr. R. Coleman (Glaxo Research Group, Ltd, Greenford, Middlesex, United Kingdom).

Support for this project was provided by NIH DK-37097 (M.D. Breyer) and a Veterans Administration merit award. Support was also provided by NIH grants DK46205 (R.M. Breyer) and funding from the Medical Research Councils and Kidney Foundation of Canada (R.L. Hébert). M.D. Breyer is a recipient of a Veterans Administration Clinical Investigator Award. R.L. Hébert was supported by funds from the Canadian Medical Research Council, and by the National Kidney Foundation.

References

1. Bonvalet, J.P., P. Pradelles, and N. Farman, 1987. Segmental synthesis and actions of prostaglandins along the nephron. *Am. J. Physiol.* 253:F377–F387.

2. Schlondorff, D. 1993. Renal complications of nonsteroidal anti-inflammatory drugs. *Kidney Int*. 44:643–653.

3. Riegger, G.A.J., D. Elsner, and E.P. Kromer. 1989. Circulatory and renal control by prostaglandins and renin in low cardiac output in dogs. *Am. J. Physiol*. 256:H1079–H1086.

4. Gurwitz, J., J. Avorn, R. Bohn, R. Glynn, M. Monane, and H. Mogun. 1994. Initiation of antihypertensive treatment during nonsteroidal anti-inflammatory drug therapy. *J. Am. Med. Assoc*. 272:781–786.

5. Murray, M., P. Breene, D. Brater, A. Manatunga, and S. Hall. 1992. Effect of flurbiprofen on renal function in patients with moderate renal insufficiency. *Br. J. Clin. Pharmacol*. 33:385–393.

6. Stokes, J.B., and J.P. Kokko. 1977. Inhibition of sodium transport by prostaglandin E2 across the isolated perfused rabbit collecting tubule. *J. Clin. Invest.* 52:1099–1104.

7. Hébert, R.L., H.R. Jacobson, and M.D. Breyer. 1991. Prostaglandin E2 inhibits sodium transport in the rabbit CCD by raising intracellular calcium. *J. Clin. Invest*. 87:1992–1998.

8. Coleman, R.A., W.L. Smith, and S. Narumiya. 1994. International union of pharmacology classification of prostanoid receptors: properties, distribution, and structure of the receptors and their subtypes. VIII. *Pharmacol. Rev*. 46: 205–229.

9. Breyer, M., H. Jacobson, and R. Breyer. 1996. Functional and molecular aspects of renal prostaglandin receptors. *J. Am. Soc. Nephrol*. 7:8–17.

10. Toh, H., A. Ichikawa, and S. Narumiya. 1995. Molecular evolution of receptors for eicosanoids. *FEBS Lett.* 361:17–21.

11. Coleman, R.A., I. Kennedy, P.P.A. Humphrey, K. Bunce, and P. Lumley. 1990. Prostanoids and their receptors. *In* Comprehensive Medicinal Chemistry. J.C. Emmet, editor. Pergammon Press. Ltd., Oxford. 643–714.

12. Watabe, A., Y. Sugimoto, A. Irie, T. Namba, M. Negishi, S. Ito, S. Narumiya, and A. Ichikawa. 1993. Cloning and expression of cDNA for a mouse EP_1 subtype of prostaglandin E receptor. *J. Biol. Chem*. 268:20175–20178.

13. Funk, C., L. Furchi, G. FitzGerald, R. Grygorczyk, C. Rochette, M.A. Bayne, M. Abramovitz, M. Adam, and K.M. Metters. 1993. Cloning and expression of a cDNA for the human prostaglandin E receptor EP_1 subtype. *J. Biol. Chem*. 268:26767–26772.

14. Båtshake, B., C. Nilsson, and J. Sundelin. 1995. Molecular characterization of the mouse prostanoid EP_1 receptor gene. *Eur. J. Biochem.* 231:809–814.

15. Lanthorn, T., R. Bianchi, and W. Perkins. 1995. EP_1 receptor antagonist blocks the diarrheagenic, but not cytoprotective, actions of a synthetic prostaglandin. *Drug Dev. Res.* 34:35–38.

16. Breyer, R., L. Davis, C. Nian, R. Redha, B. Stillman, H. Jacobson, and M. Breyer. 1996. Cloning and expression of the rabbit prostaglandin EP_4 receptor. *Am. J. Physiol.* 270:F485–F493.

17. Breyer, M. 1991. Feedback inhibition of cyclic adenosine monophosphate stimulated Na transport in the rabbit cortical collecting duct via Na^+ dependent basolateral Ca^{++} entry. *J. Clin. Invest*. 88:1502–1510.

18. Bastien, L., N. Sawyer, R. Grygorczyk, K. Metters, and M. Adam. 1994. Cloning, functional expression, and characterization of the human prostaglandin E_2 receptor EP_2 subtype. *J. Biol. Chem*. 269:11873–11877.

19. Honda, A., Y. Sugimoto, T. Namba, A. Watabe, A. Irie, M. Negishi, S. Narumiya, and A. Ichikawa. 1993. Cloning and expression of a cDNA for mouse prostaglandin E receptor EP2 subtype. *J. Biol. Chem*. 268:7759–7762.

20. Namba, T., Y. Sugimoto, M. Negishi, A. Irie, F. Ushikubi, A. Kakizuka, S. Ito, A. Ichikawa, and S. Narumiya. 1993. Alternative splicing of C-terminal tail of prostaglandin E receptor subtype EP3 determines G-protein specificity. *Nature*. 365:166–170.

21. Regan, J.W., T.J. Bailey, D.J. Pepperl, K.L. Pierce, A.M. Bogardus, J.E. Donello, C.E. Fairbairn, K.M. Kedzie, D.F. Woodward, and D.W. Gil. 1994. Cloning of a novel human prostaglandin receptor with characteristics of the pharmacologically defined EP2 subtype. *Mol. Pharmacol.* 46:213–220.

22. Sugimoto, Y., T. Namba, M. Negishi, A. Ichikawa, and S. Narumiya. 1992. Cloning and expression of a cDNA for mouse prostaglandin E receptor EP3 subtype. *J. Biol. Chem*. 267:6463–6466.

23. Breyer, R.M., R.B. Emeson, M.D. Breyer, R.M. Abromson, L.S. Davis, and S.M. Ferrenbach. 1994. Alternative splicing generates multiple isoforms of a rabbit prostaglandin E2 receptor. *J. Biol. Chem*. 298:6163–6169.

24. Sugimoto, Y., T. Namba, R. Shigemoto, M. Negishi, A. Ichikawa, and S. Narumiya. 1994. Distinct cellular localization of mRNAs for three subtypes of prostaglandin E receptor in kidney. *Am. J. Physiol*. 266:F823–F828.

25. Sakairi, Y., H.R. Jacobson, T.D. Noland, and M.D. Breyer. 1995. Luminal prostanglandin E receptors regulate salt and water transport in rabbit cortical collecting duct. *Am. J. Physiol*. 269:F257–F265.

26. Hébert, R.L., H.R. Jacobson, D. Fredin, and M.D. Breyer. 1993. Evidence that separate PGE2 receptors modulate water and sodium transport in rabbit cortical collecting duct. *Am. J. Physiol*. 265:F643–F650.

27. Hébert, R., L. Regnier, and L. Peterson. 1995. Rabbit cortical collecting ducts express a novel prostacyclin receptor. *Am. J. Physiol.* 268:F145–F154.

28. Breyer, M., L. Davis, H. Jacobson, and R. Breyer. 1996. Differential localization of prostaglandin E receptor subtypes in human kidney. *Am. J. Physiol.* 270:F912–F918.

29. Okuda-Ashitaka, E., K. Sakamoto, T. Ezashi, K. Miwa, S. Ito, and O. Hayashi. 1996. Suppression of prostaglandin E receptor signaling by the variant form of EP_1 subtype. *J. Biol. Chem.* 271:31255–31261.

30. Guan, Y., M. Chang, W. Cho, Y. Zhang, R. Redha, L. Davis, S. Chang, R. Dubois, C.-M. Hao, and M. Breyer. 1997. Cloning, expression, and regulation of rabbit cyclooxygenase-2 in renal medullary interstitial cells. *Am. J. Physiol*. 273:F18–F26.

31. Schuster, V.L. 1985. Mechanism of bradykinin, ADH, and cAMP interaction in rabbit cortical collecting duct. *Am. J. Physiol.* 249:F645–F653.

32. Berlin, T., R. Cronestrand, J. Nowak, T. Sonnenfeld, and A. Wennmalm. 1979. Conversion of arachidonic acid to prostaglandins in homogenates of human skeletal muscle and kidney. *Acta. Physiol. Scand.* 106:441–445.

33. Sedor, J.R., E.W. Davidson, and M.J. Dunn. 1986. Effects of nonsteroidal anti-inflammatory drugs in healthy subjects. *Am. J. Med.* 81(Suppl. 2B):58–70.

34. Grynkiewicz, G., M. Poenie, and R.Y. Tsien. 1985. A new generation of Ca^{2+} indicators with greatly improved fluorescence properties. *J. Biol. Chem*. 260:3440–3450.

35. Kiriyama, M., F. Ushikubi, T. Kobayashi, M. Hirata, Y. Sugimoto, and S. Narumiya. 1997. Ligand binding specificities of the eight types and subtypes of the mouse prostanoid receptors expressed in Chinese hamster ovary cells. *Br. J. Pharmacol*. 122:217–224.

36. Abramovitz, M., Y. Boie, T. Nguyen, T.H. Rushmore, M.A. Bayne, K.M. Metters, D.M. Slipetz, and R. Grygorczyk. 1994. Cloning and expression of a cDNA for the human prostanoid FP receptor. *J. Biol. Chem*. 269:2632–2636.

37. Dunn, M.J., and V.L. Hood. 1977. Prostaglandins and the kidney. *Am. J. Physiol*. 233:F169–F184.

38. Naray-Fejes-Toth, A., G. Fejes-Toth, C. Fischer, and J. Frolich. 1984. Effect of dexamethasone on in vivo prostanoid production in the rabbit. *J. Clin. Invest*. 74:120–123.

39. Johnston, H.H., J.P. Herzog, and D.P. Lauler. 1967. Effect of prostaglandin E on renal hemodynamics, sodium, and water excretion. *Am. J. Physiol*. 213:939–946.

40. Iino, Y., and M. Imai. 1978. Effects of prostaglandins on sodium transport in isolated collecting tubules. *Pflugers Arch.* 373:125–132.

41. Ling, B., K. Kokko, and D. Eaton. 1992. Inhibition of apical Na^+ channels in rabbit cortical collecting tubules by basolateral prostaglandin E2 is modulated by protein kinase C. *J. Clin. Invest.* 90:1328–1334.

42. Frindt, G., and E.E. Windhager. 1990. $Ca2^+$-dependent inhibition of sodium transport in rabbit cortical collecting tubules. *Am. J. Physiol*. 258:F568–F582.

43. Breyer, M., and Y. Ando. 1994. Hormonal signaling and regulation of salt and water transport in the collecting duct. *Annu. Rev. Physiol.* 56:711–739.

44. Nemoto, K., C.C. Pilbeam, S. Bilak, and L. Raisz. 1997. Molecular cloning and expression of the rat prostaglandin E2 receptor of the EP2 subtype. *Prostaglandins.* 54:713–725.

45. Breyer, M.D., H.R. Jacobson, L.S. Davis, and R.M. Breyer. 1993. In situ hybridization and localization of mRNA for the rabbit prostaglandin EP3 receptor. *Kidney Int.* 43:1372–1378.

46. Båtshake, B., and J. Sundelin. 1996. The mouse genes for the EP_1 prostanoid receptor and the PKN protein kinase overlap. *Biochem. Biophys. Res. Commun.* 227:70–76.

47. Abramovitz, M., M. Adam, Y. Boie, R. Grygorczyk, T. Rushmore, T. Nguyen, C. Funk, L. Bastien, N. Sawyer, C. Rochette, et al. 1995. Human prostanoid receptors: cloning and characterization. *Adv. Prostaglandin Thromboxane Leukotriene Res*. 23:499–504.

48. Morimoto, M., Y. Sugimoto, M. Katsuyama, H. Oida, K. Tsuboi, K. Kishi, Y. Kinoshita, M. Negishi, T. Chiba, S. Narumiya, and A. Ichikawa. 1997. Cellular localization of mRNAs for prostaglandin E receptor subtypes in mouse gastro-intestinal tract. *Am. J. Physiol.* 272:G681–G687.

49. Oka, T., and T. Hori. 1994. EP_1 receptor mediation of prostaglandin E_2–induced hyperthermia in rats. *Am. J. Physiol.* 267:R289–R294.

50. Audoly, L., and R. Breyer. 1997. The second extracellular loop of the prostaglandin EP3 receptor is an essential determinant of ligand selectivity. *J. Biol. Chem*. 272:13475–13478.

51. Audoly, L., and R. Breyer. 1997. Substitution of charged amino acid residues in transmembrane regions 6 and 7 affect ligand binding signal transduction of the prostaglandin EP3 receptor. *Mol. Pharmacol.* 51:61–68.